Structural dynamics of flexible rotor blades to study aeroelastic phenomena

Anais Chambon, Leonardo Sanches, Sébastien Prothin, Christophe Eloy, Guilhem Michon

Structural dynamics of flexible rotor blades to study aeroelastic phenomena

A. Chambon*
ISAE-Supaero, 10 Avenue Edouard Belin, 31400 Toulouse, France

L. Sanches†
Université de Toulouse, ICA, CNRS, ISAE-Supaero, 10 Avenue Edouard Belin, 31400 Toulouse, France

S. Prothin‡
ISAE-Supaero, 10 Avenue Edouard Belin, 31400 Toulouse, France

C. Eloy§
IRPHE, Aix Marseille Université, CNRS, Centrale Marseille, 49 rue F.Joliot Curie, 13013, Marseille, France

G. Michon¶
Université de Toulouse, ICA, CNRS, ISAE-Supaero, 10 Avenue Edouard Belin, 31400, Toulouse, France

Nowadays, experimental analyses of fluid-structure interactions on flexible rotating blades are few widespread. For this purpose, an experimental rotor test bench for blades with variable flexibility is under development. Different sets of blades have been fabricated with different composite materials and variable thickness, depending on the number of layers considered. The main objective of the present work is to estimate which sets of blades are more sensitive to flutter occurrence based on their Campbell diagrams.
For this purpose, a finite element approach is developed to model the dynamic behavior of the blades assumed as a uniform, slender, isotropic and homogeneous beam with out-of-plane bending and torsion deformations, submitted to inertial and centrifugal forces due the rotation effects. Two numerical models were developed by considering Timoshenko and Euler-Bernoulli beam theories; both are validated by means of the software COMSOL®.
Later, the mechanical properties of each set of blades have been identified from the frequency response functions (FRFs) obtained through experimental vibration tests. The frequencies and eigenmodes of blades determined experimentally are compared with those obtained with FEM model. Then, rotation effects on the blade frequencies are studied by using Campbell diagrams for all set of blades studied. It is evidenced for some of the sets the presence of intersections between bending and torsional frequencies in the interval of the operational rotating speed of the test bench. This fact might be considered as an indicator of potential flutter occurrence. Aerodynamic load will be consider in the future work.

I. Nomenclature

DOF	=	Degree of freedom abbreviation
EB	=	Euler-Bernoulli abbreviation
EOM	=	Equation of motion
FEM	=	Finite Element Method abbreviation
GVT	=	Ground vibration test
Tim	=	Timoshenko abbreviation

*PhD student, anais.chambon@isae-supaero.fr.
†Research scientist, Leonardo.SANCHES@isae-supaero.fr.
‡Research scientist, Sebastien.Prothin@isae-supaero.fr.
§Professor, IRPHE, christophe.eloy@irphe.univ-mrs.fr.
¶Research director, Guilhem.Michon@isae-supaero.fr, AIAA Member.

A				=	Cross-sectional area for a rectangular section, $[m^2]$
E				=	Young's modulus, $[Pa]$
G				=	Shear modulus, $[Pa]$
$\mathbf{G}$				=	Global gyroscopic matrix
H_1,	H_2,	H_3,	H_4	=	Hermite cubic polynomial shape functions
I_y				=	Second moment of inertia about the y-axis, $[m^4]$
I_z				=	Second moment of inertia about the z-axis, $[m^4]$
I_α				=	Mass moment of inertia about elastic axis $[m^4]$
J				=	Polar moment of inertia, $[m^4]$
k				=	Shear correction factor
$\mathbf{K}$				=	Global stiffness matrix
L				=	Total length of the beam, $[m]$
l_i				=	Length of a beam element, $[m]$
$\mathbf{M}$				=	Global mass matrix
N_1,	N_2			=	Linear shape functions
$\mathbf{q}$				=	Degrees of freedom vector
T				=	Kinetic energy, $[J]$
T_c				=	Centrifugal force, $[N]$
U				=	Potential energy, $[J]$
w				=	Flap deflection DOF
x, y, z				=	Global coordinate axis system
ρ				=	Density, $[kg/m^3]$
Ω				=	Rotating speed of the blade, $[rad/s]$
φ				=	Bending slope (rotation) DOF
ψ				=	Torsion DOF

II. Introduction

According to Collar's definition [1], aeroelasticity is the result of interactions between elastic forces of a structure and inertial forces of a fluid. Summarized a Fluid Structure Interaction phenomenon (FSI). In the case of rotating flexible blades, the structural properties of the blade determine the main modes of bending and twisting. For some operating points (i.e. for certain rotation speed), these modes may be excited and lead to different instabilities phenomenon such as aeroelastic flutter. It is an unsteady self-excited vibration, in which the structure exchanges energy with the flow. One of the causes of this phenomenon is the coalescence of two structural modes: Flexion and torsion, which reach the same vibration frequency. In this case, the blade vibrates uncontrollably and aerodynamic performance is severely degraded. This problem is general to rotors. However, it takes an even more significant scale in the context of passively adaptive blades (the blade is deformed under the centrifugal effect of rotation) due to the flexibility of the blades. One of the consequences of these instabilities is the instantaneous or fatigue structural damage on the system. The interest of understanding and controlling this phenomenon is therefore essential. However, FSI analyses are computationally strongly expensive, that's why it is necessary to find a trade off between accuracy and cost. From the first steps in the study of this type of phenomena, simplified and analytical models have been developed and have proven their efficiency in the modeling of these instabilities. Indeed, J.Sicard [2] investigated the aeroelastic stability of a flexible ribbon rotor blade by using an Euler-Bernoulli beam theory including large twist angles and unsteady aerodynamics including the effect of returning wake with Loewy theory. In this study, the analysis is validated with the experimental measurements and flutter boundaries are identified.

More recently, S.Shams [3] applied unsteady aerodynamic empirical models as Theodorsen and Loewy together with blade element momentum theory to analyze the aeroelastic stability of a wind turbine blade section. Besides, they investigated the effects of different parameters on flutter boundaries.

E.Durán Venegas [4] described a fluid-structure model for flexible rotor blades. The blade deformation is obtained by solving the nonlinear equations for bending and twisting angles from a one-dimensional beam model.

In this work, beam models have been used to study the vibratory behavior of flexible blades in rotation. In parallel, an experimental rotor test bench is under development. Several sets of blades with different material properties have been designed for this test bench. In order to identify which type of blades would be more sensitive to flutter, by considering the Campbell diagrams obtained for the different sets of blades.

In section III, a numerical FEM model of a rotating slender beam, undergoing out-of-plane bending and Torsion deformations has been developed. Timoshenko and Euler-Bernoulli beam theories were considered and validated by means of a commercial numerical software COMSOL®. Centrifugal effects were added to the existent non-rotating beam validated model, to study the behavior of the blades subjected to rotating speed. In section IV, different sets of blades with variable flexibility have been designed, for the experimental rotor test bench under development. Mechanical characterization of the blades has been performed from experimental vibration tests. Then, the effects of the rotation are studied by using Campbell diagrams of all sets of blades.
The conclusions and prospects are presented in the last section.

III. Structural model

Conventional rotor blades are generally long, thin structures that can be modeled as beams. R. Bielawa [5] and D. Hodges [6] described the concepts relating to blade vibration, including beam theories and FEM.
Several beam theories have been developed and are still widely used. One of these first theories is called Euler-Bernoulli beam theory. The main assumptions are that the cross-section of the beam is assumed to be rigid (i.e, no deformations occur in the plane of the cross-section), shear deformations and rotary inertia are neglected. The cross section remains plane after deformation, unstretched and normal to the deformed axis of the beam. Timoshenko beam theory is mostly used in the case of short or thick beam where shear effects can be significant. This theory includes the effect of shear deformation and inertia of rotation. As a result, the difference in Timoshenko theory is that after deformation, the cross-section of the beam is no more normal to the beam axis.

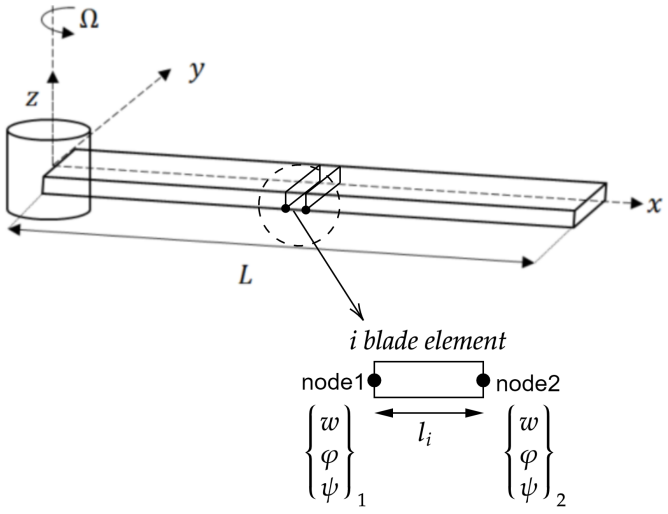

Fig. 1 Coordinate system and degrees of freedom of a beam finite element.

A global coordinate system (x, y, z) shown in Fig . 1 is used for the description of the blade geometry. In the finite element approach, forces and moments are applied to the nodes of the elements. Fig . 1 depict a blade of length L rotating at Ω around z axis, discretized as beam elements with 2 nodes on each element. Each node of these beam elements are submitted to 3 degrees of freedom (DOF), out-of-plane deflection $w(x,t)$, its respective slope (rotation) $\varphi(x,t)$ and torsion angle $\psi(x,t)$. No in-plane bending and radial displacements are considered. These DOF can be expressed by means of Shape Functions (Interpolation functions), which describes these movements. Thus, Hermite cubic polynomial and linear shape functions have been used to approximate the flexural and torsional displacements of the beam, respectively.

The first objective of this mechanical model is to study the dynamic behavior of a blade. It is based on a finite isotropic beam element model, of an homogeneous, slender beam of rectangular cross-section undergoing bending and torsion deformations. Thus giving access to the natural frequencies and the modes of the blades.
In Table. 1, the frequencies obtained with the two developed models in bending (F) and torsion (T) based on the Timoshenko and Euler-Bernoulli beam theories and with COMSOL® are compared. "COMSOL Beam element" model correspond to the COMSOL finite element model expressed with beam elements. While "COMSOL Beam solid (3D)" model, considers 3D solid elements. The latter allows to obtain the Torsional frequencies of the beam, contrary to the

COMSOL beam element model.
According to Table. 1 there's no difference between results obtained with the two developed models for a thin rectangular cross-section. Respective frequencies of each models are close, Flexural frequencies of the COMSOL beam model and the one developed are identical. Moreover, frequencies of COMSOL 3D model presents good accuracy with FEM beam code developed, in bending and torsion.

Table 1 Frequencies of a Cantilever beam with rectangular section, for Timoshenko (TIM) and Euler-Bernoulli (EB) theories.

Modes	Frequencies, Hz				
	FEM Beam code		COMSOL Beam element		COMSOL Beam solid (3D)
	TIM	EB	TIM	EB	
ω_1, F	5.2	5.2	5.2	5.2	5.2
ω_2, F	32.4	32.4	32.4	32.4	32.7
ω_3, T	79.3	79.3	-	-	81.8
ω_4, F	90.6	90.6	90.6	90.6	92.0
ω_5, F	177.5	177.5	177.5	177.5	181.0
ω_6, T	238.0	238.0	-	-	247.5

According to the previous Table of frequencies, Euler-Bernoulli may be sufficient for this study. However, it could be relevant to use these two beam assumptions, because it will allows to adapt the model more generally to other types of beams (thick).

Then, it is necessary to add centrifugal effects in this study in order to model the behavior of the blades subjected to rotating speed and to identify its effects on the natural frequencies of the beams. This analysis and some of these results will be detailed in the section IV.
By using the interpolation functions and by introducing them into the Lagrange equations, the expressions of kinetic and Potential energies of a cantilever rotating beam are obtained and shown respectively in, Eq. (1) and Eq. (2):

$$T = \frac{1}{2}\int_0^L \left\{\rho A\dot{w}^2 + \rho I_y\left[\Omega^2\varphi^2 + \dot{\varphi}^2 + 2\Omega(\varphi\dot{\psi} - \dot{\varphi}\psi)\right] + I_\alpha\dot{\psi}^2 + \rho(I_y - I_z)\Omega^2\psi^2 + 2\rho I_z\Omega(\varphi\dot{\psi} - \dot{\varphi}\psi)\right\} dx \tag{1}$$

$$U = \frac{1}{2}\left[\int_0^L \left\{EI_y(\varphi')^2 + T_c\left[(w')^2 + \frac{I_\alpha}{\rho A}(\psi')^2\right] + kAG(w' - \varphi)^2 + GJ(\psi')^2\right\} dx\right] \tag{2}$$

The Energy equations written above are defined in the case of a Timoshenko beam theory. It is possible to activate or desactivate terms related to Timoshenko beam theory (i.e rotary inertia and shear effect) to get the Euler-Bernoulli equations. It allows to build the elementary mass, gyroscopic and stiffness matrices, essential in the implementation of a finite element model.
Then the governing equations of motion of a rotating cantilever beam can be derived by using Hamilton's principle, as Eq. (3)

$$\mathbf{M}\ddot{\mathbf{q}} + \mathbf{G}\dot{\mathbf{q}} + \mathbf{K}\mathbf{q} = 0 \tag{3}$$

with **M**, **G** and **K** respectively, the mass matrix, the gyroscopic matrix, the stiffness matrix. The vector **q** contains all the DOF of the elements used to model the rotating beam.

IV. Experimental dynamical characterization of flexible blades

Composite flexible blades are designed and manufactured by considering different materials and geometric aspects to study aeroelastic phenomena of rotating blades on dedicated experimental setup under development. The main

objective of the present work is to estimate which sets of blades are potential candidates based on their Campbell diagram. For this purpose, in the present section, the mechanical properties of each set of blades are identified from the frequency response functions (FRFs) measured through experimental vibration tests.

Among the manufactured blades, carbon and fiberglass composite materials are used under different configuration sets as function of the number of fiber oriented plies considered (stacking sequence). In addition, several sets of length (i.e.: aspect ratio) is considered too. Table. 2 gives an example of the set of blades studied. Many more configurations have been studied, but are not presented in this abstract. The set of blades named AR8-L8 means that 8 plies is considered for the composite structure and with an aspect ratio (AR) of 8. All blades have the same width of 5cm while the thickness is function of the layers quantity considered. For all set of blades fabricated, a quasi-isotropic hypothesis is assumed for modelling purposes.

Table 2 Mechanical properties of two experimental blades.

Name	Material	Blade chord (mm)	Blade length (mm)	Aspect Ratio (AR)	Stacking sequence	E $[GPa]$	G $[GPa]$
AR8	Carbon	50	400	8	[90/-45/0/90/45/0]s	38.89	8.90
AR8-L8	Fiberglass	50	400	8	[0/45/90/-45]s	17.95	5.59

Experimental modal analysis of each set of blades is carried out for characterization and identification of their mechanical properties. The vibration test consists in a base excitation condition of a blade mounted (clamped) in a support. A scanning vibrometer laser is used to map out the vibrating response of the blade at different positions as it shown in Figure . 2. In this configuration, mostly the bending vibration modes are highlighted. L. Bernard [7] described the vibration test procedure for a sandwich composite beam in order to test the bending-torsion coupling. For investigating the torsional modes, an impact hammer is used for a non-symmetrical excitation load. Major specifications about the experimental procedure used, will be detailed in the final version of this paper. Figure . 3 shows the FRFs obtained for the configuration AR8-L8 under base and hammer impact conditions.

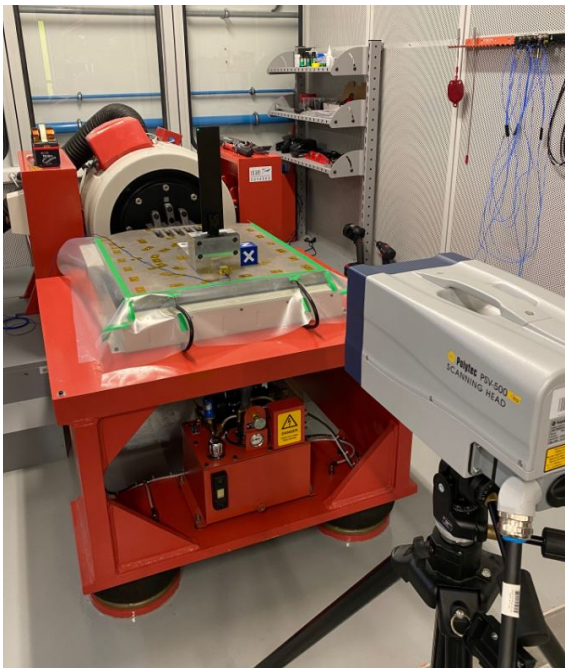

Fig. 2 Ground vibration test of an experimental blade.

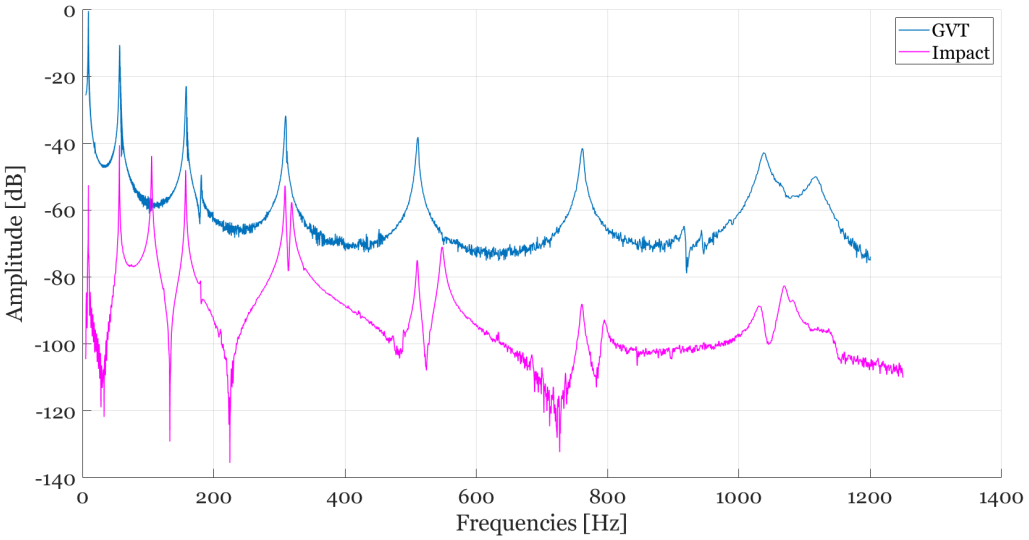

Fig. 3 FRF signals of a hammer impact (pink) and GVT (blue) for AR8-L8 configuration.

The identification of the mechanical properties are done by minimizing the error between the natural frequencies determined with the FRFs and those computed with the developed FEM. An optimisation procedure is implemented to identify the equivalent isotropic Young and Shear modulus, as it is shown in the two last columns of Table 2. Table 3 summarises the results obtained for AR8-L8 blade configuration. The good agreement between results is observed and it shows a good accuracy of the optimized parameters in the present FEM model.

Table 3 Bending and Torsional FEM model and experimental frequencies of AR8-L8 configuration Blade.

Models \ Frequencies (Hz)	ω_1, F	ω_2, F	ω_3, T	ω_4, F	ω_5, F	ω_6, T
Experimental	7.40	57.11	105.47	157.60	309.56	318.75
Beam FEM (E,G Optim)	8.83	55.31	106.63	154.90	303.49	320.19
Relative difference (%)	19.3 %	3.2 %	1.1 %	1.7 %	2.0 %	0.5 %

Campbell diagrams are then studied by considering the effects of the rotating blade. Indeed, dynamical efforts acting in the blade affects its vibrating properties. Figure . 4 illustrates the evolution of the natural frequencies with the increase of the rotating speed for AR8 (stiffer) and AR8-L8 configurations.

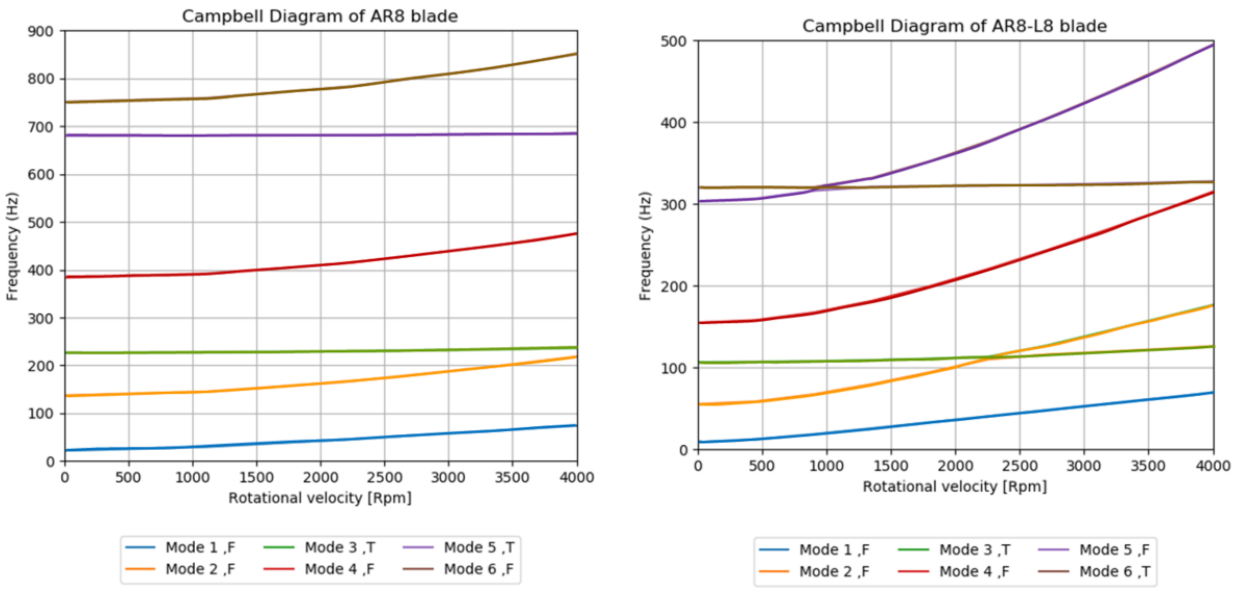

Fig. 4 Campbell Diagrams of a rigid AR8 blade (left) and a flexible AR8-L8 blade (right), without aerodynamic effects.

Campbell diagrams in Figure . 4 highlights intersection points of the bending and torsional frequencies for the flexible blade (AR8-L8) for rotating speed lower than 4000 rpm. Nonetheless, no intersection is observed for the stiffer blade (AR8), in this speed range.

These intersections of bending and torsional frequencies are indicators of potential flutter occurrence. This analysis is carried out for the all set of blades and it allows to understand the the effects of aspect ratio and composite layers on the potential flutter occurrence. For instances, the set AR8-L8 is a potential candidate for the experimental aeroelastic setup of rotating blade under development (maximum rotating speed of 4000 rpm).

V. Conclusion

The blades were manufactured, responding to the limitations of the rotor test bench and the considerations of the model. A mechanical dynamic characterization of all the blade sets have been established, allowing the identification of the material parameters of the blades. In addition, a beam model with 3 DOF was developed and validated numerically with COMSOL in the case of Euler-Bernouli and Timoshenko beam theories, but also with the vibration tests carried out on the blades. Campbell diagrams of all the blade sets have been drawn up, allowing to model the behavior of the blades submitted to rotation speed, without aerodynamic load. They shows interactions between bending and torsional frequencies, which can be indicators of potential flutter occurrence.

Then, with the experimental rotor test bench under development, it will be possible to analyze the coupled FSI phenomenon, for some operating speeds and for some sets of blades. A comparative analysis of the results discussed in the final paper and the experimental study of the rotor will be held, in order to link with the results of studies carried out on fixed blades.

References

[1] Collar, A. R., "The Expanding Domain of Aeroelasticity," *The Journal of the Royal Aeronautical Society*, Vol. 50, No. 428, 1946, pp. 613–636. https://doi.org/10.1017/S0368393100120358, URL https://www.cambridge.org/core/product/identifier/S0368393100120358/type/journal_article.

[2] Sicard, J., and Sirohi, J., "Aeroelastic stability of a flexible ribbon rotor blade," *Journal of Fluids and Structures*, Vol. 67, 2016, pp. 106–123. https://doi.org/10.1016/j.jfluidstructs.2016.09.010, URL https://linkinghub.elsevier.com/retrieve/pii/S0889974616301803.

[3] Shams, S., and Esbati Lavasani, R., "Aeroelastic stability analysis of a wind turbine blade section with trailing edge flap using a

flexible unsteady blade elements momentum theory," *Journal of the Brazilian Society of Mechanical Sciences and Engineering*, Vol. 41, No. 8, 2019, p. 324. https://doi.org/10.1007/s40430-019-1789-5, URL http://link.springer.com/10.1007/s40430-019-1789-5.

[4] Durán Venegas, E., Le Dizès, S., and Eloy, C., "A strongly-coupled model for flexible rotors," *Journal of Fluids and Structures*, 2019, p. S0889974618309393. https://doi.org/10.1016/j.jfluidstructs.2019.03.022, URL https://linkinghub.elsevier.com/retrieve/pii/S0889974618309393.

[5] Bielawa, R. L., *Rotary wing structural dynamics and aeroelasticity*, 2nd ed., Education series, American Institute of Aeronautics and Astronautics, Reston, Va, 2006. OCLC: 836251633.

[6] Hodges, D. H., and Pierce, G. A., *Introduction to structural dynamics and aeroelasticity*, 2nd ed., No. 15 in Cambridge aerospace series, Cambridge Univ. Press, New York, NY, 2011.

[7] Bernard, L., Michon, G., El Fatmi, R., and Castanié, B., "Static and dynamic analysis of bending–torsion coupling of a CFRP sandwich beam," *Composite Structures*, Vol. 145, 2016, pp. 26–36. https://doi.org/10.1016/j.compstruct.2016.02.055, URL https://linkinghub.elsevier.com/retrieve/pii/S0263822316300964.